Supporting Information

Single-Drop Solution Electrode Discharge-Induced Cold Vapor Generation Coupling to Matrix Solid-Phase Dispersion: A Robust Approach for Sensitive Quantification of Total Mercury Distribution in Fish

Qian Chen[†], Yao Lin[†], Yunfei Tian[‡], Li Wu[‡], Lu Yang[§], Xiandeng Hou[†,‡], and Chengbin Zheng[†*]

[†] Key Laboratory of Green Chemistry & Technology of MOE, College of Chemistry, Sichuan University, Chengdu, Sichuan 610064, China

[‡]Analytical & Testing Center, Sichuan University, Chengdu, Sichuan 610064, China

[§] National Research Council Canada, Ottawa, Ontario K1A 0R6, Canada

*Corresponding author:

Fax: +86 28 85412907; Phone: +86-28-85415810

E–mails: abinscu@scu.edu.cn (C. B. Zheng)

Author Contributions

The manuscript was written through contributions of all authors. All authors have given approval to the final version of the manuscript.

Table of Content

1. The Optimum Parameters for AFS

Table S1. Operation Conditions of AFS

Parameter	Value
Hollow cathode lamp	Hg (253.7 nm)
Lamp current, mA	80
Voltage for photomultiplier tube, V	-280
Observation height, mm	10
Carrier Ar flow rate, mL min^{-1}	500
Shield Ar flow rate, mL min^{-1}	1000
Quantification mode	Peak area

2. The Photographs of the Organs of Common Carp.

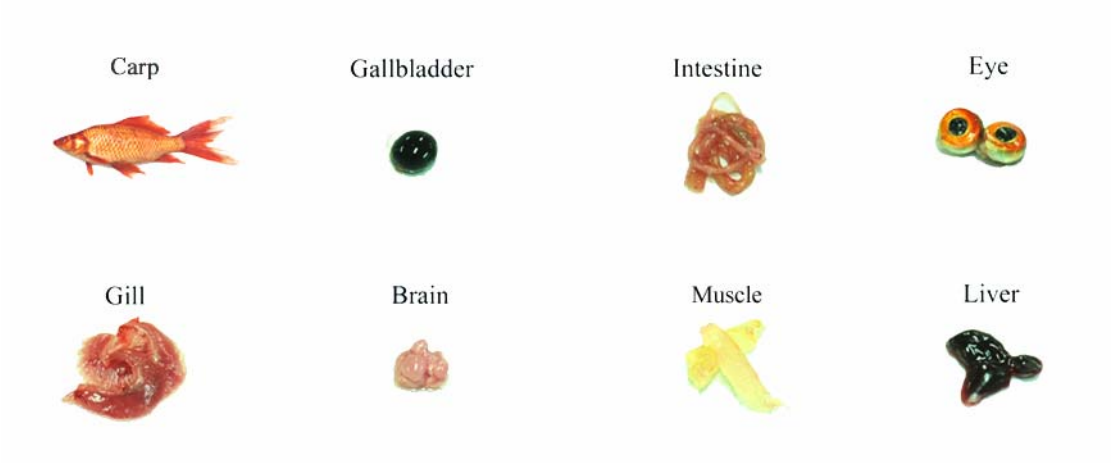

Figure S1. The photographs of the organs of common carp

3. Optimization of SD-SEGD-CVG.

3.1. Effect of the Ar discharge gas. In this current work, Ar gas simultaneously acts as discharge gas to generate and maintain the glow discharge, and as carrier gas to transfer the generated Hg^0 to the AFS detector. Therefore, the Ar discharge gas flow rate significantly affected the mercury response because of its significant effects on the stability of the plasma, analyte concentration in the carrier gas, analyte transport efficiency, as well as analyte residence time in the atomizer, as shown in Figure S2A. Stable plasma and efficient separation and transport of Hg^0 could not be obtained if the Ar flow rate was lower than 300 mL min^{-1}. On the other hand, significant dilution effect occurred at higher flow rates with decreased response. Therefore, an Ar flow rate of 500 mL min^{-1} was selected in all subsequent experiments to obtain the maximum response.

3.2. Effect of Discharge Voltage. In our previous work, the CVG efficiencies of Cd(II) and Zn(II) were significantly affected by discharge voltage. Therefore, the effect of discharge voltage on response of Hg was investigated in a range of 40 - 80 V. The results are summarized in Figure S2B. Response of mercury is increased with voltage increased from 40 to 60 V, followed by a plateau at higher voltages. The discharge plasma could not be generated when the voltage was lower than 40 V. Thus, a discharge voltage of 60 V was chosen for all subsequent experiments.

3.3. Effect of Discharge Gap. The discharge gap is the distance between the surface of the liquid drop and the tip of tungsten electrode, which significantly affects the generation and stability of the microplasma. The effect of discharge gap on mercury chemical vapor generation is summarized in Figure S2C. The results show that the optimal discharge gap is about 2 mm. When the gap is smaller than 0.5 mm, the barrier was broken up and the drop suddenly collapsed, thereby resulting in inefficient chemical vapor generation. The plasma was unstable and extinguished once the gap is larger than 5 mm.

3.4. Effect of Formic Acid. The effect of formic acid concentration on SD-SEGD-CVG is similar to those reported in photochemical vapor generation (PVG), DBD plasma CVG. Figure S2D reveals that the response increased

significantly with increasing concentration of formic acid in the range 0 - 1% (v), followed by a slight decrease at higher concentrations. A 4% (v/v) formic acid medium was thus used for all subsequent experiments. The concentrations of the selected chemicals are much lower than those of $SnCl_2$-HCl and THB-HCl system, significantly reducing waste and blank value.

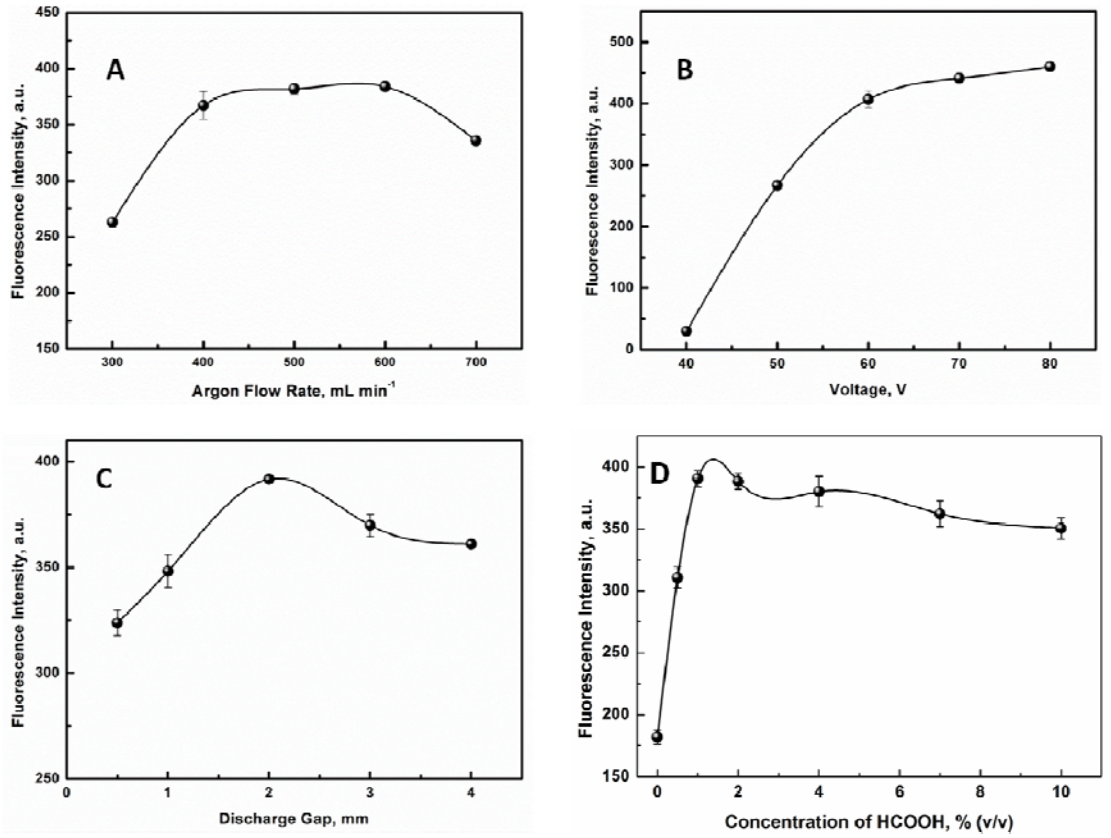

Figure S2. Optimization of the operation parameters of SD-SEGD-CVG: (A) effect of Argon flow rate; (B) effect of voltage; (C) effect of discharge gap; (D) effect of formic acid concentration

4. Optimization of MWCNTs Assisted Matrix Solid Phase Dispersion

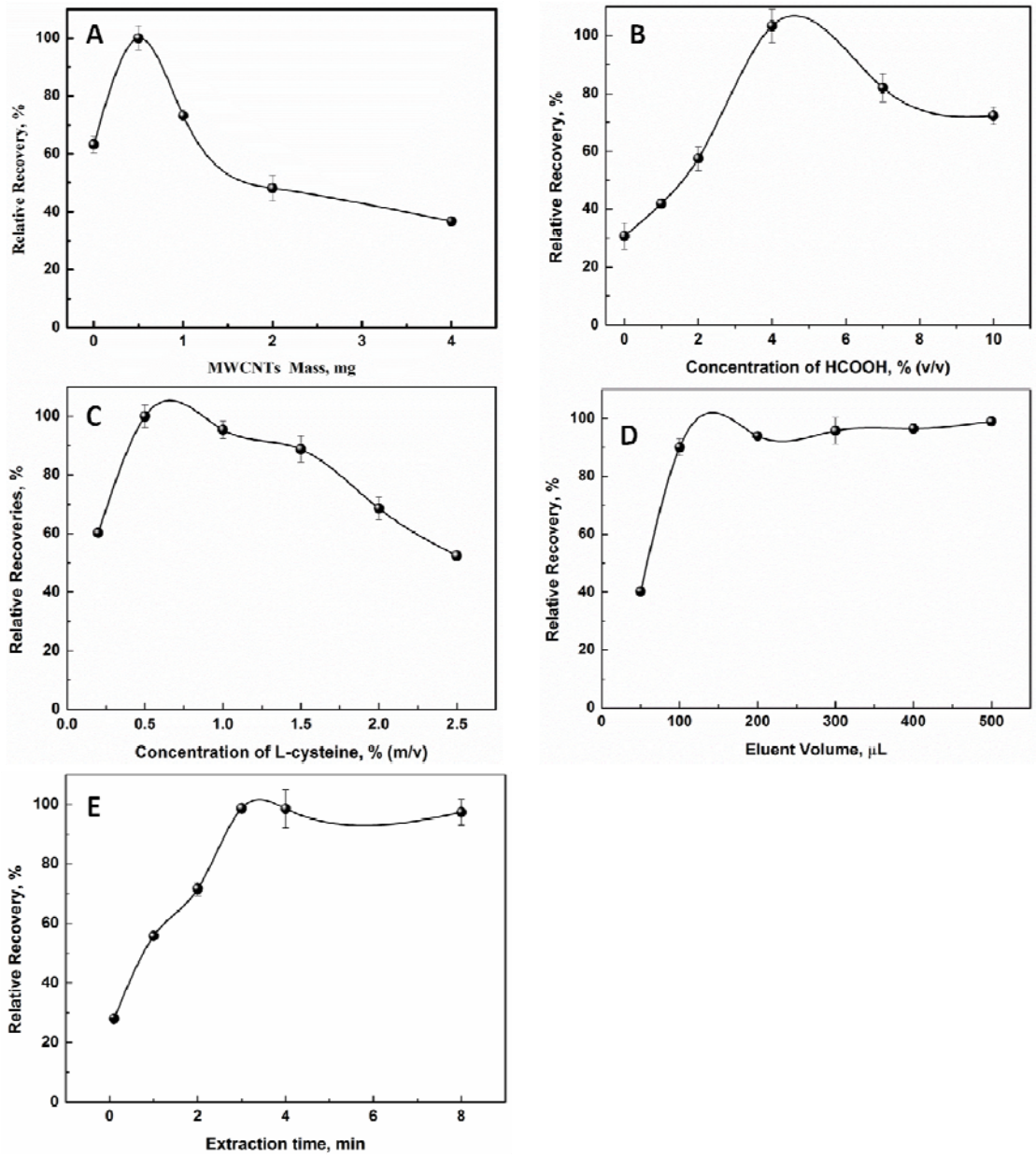

Figure S3. Effects of the experimental conditions of MWCNTs assisted MSPD on the extraction efficiency of mercury from DORM-2. (A) Mass of MWCTs, (B) concentration of HCOOH, (C) concentration of L-cysteine; (D) volume of eluent; and (D) extraction time.

5. Effect of L-cysteine Concentration of CVG Efficiency of Mercury by FI-SD-SEGD-CVG and Extraction Efficiency of Mercury from DORM-2

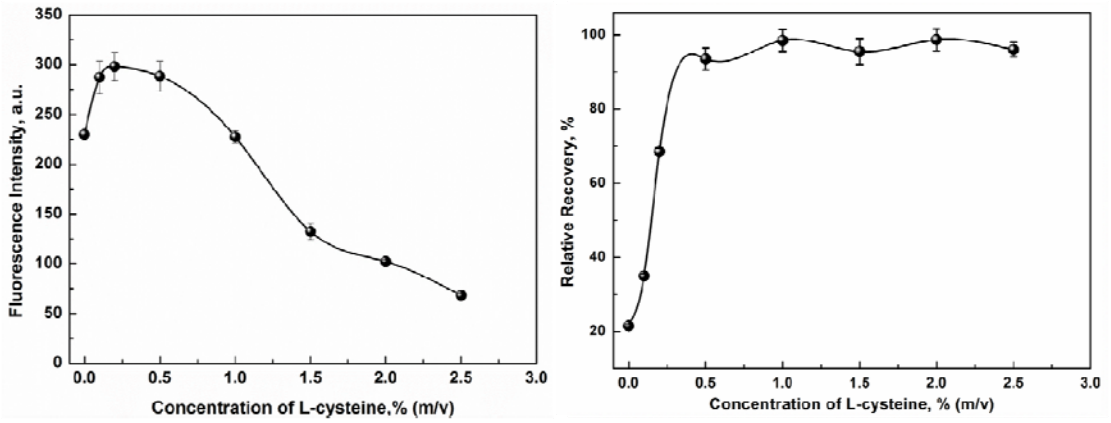

Figure S4. Effect of L-cysteine concentration on FI-SD-SEGD-CVG of mercury (left); Effect of L-cysteine concentration on extraction recoveries of mercury from DORM-2, analyzed by pneumatic nebulization ICP-MS.

6. Interference of Coexisting Ions

Many studies reported that severe suppression on CVG of mercury was found in the presence of Cl^- because it was favourable to generate strong complexes of Hg^{2+} and Cl^-.[1,2] Meanwhile, during the extraction process, L-cysteine can react with other metallic ions such as Cu^{2+} and Ag^+, which may affect the extraction of mercury from sample. The effects of 12 ions on CVG of 10 μg L^{-1} Hg^{2+} were investigated, as shown in Figure S5. The results show that no significant interferences from the tested ions occurred even at concentration as high as 10 mg L^{-1}, except Ag^+. The recovery of mercury decreased to 68% at 10 mg L^{-1} of Ag^+, which may attributed to the formation of silver amalgam under this conditions. Note that the severe suppression of Cl^- was not detected with the proposed method, even at the concentration as high as 10 mg L^{-1}.

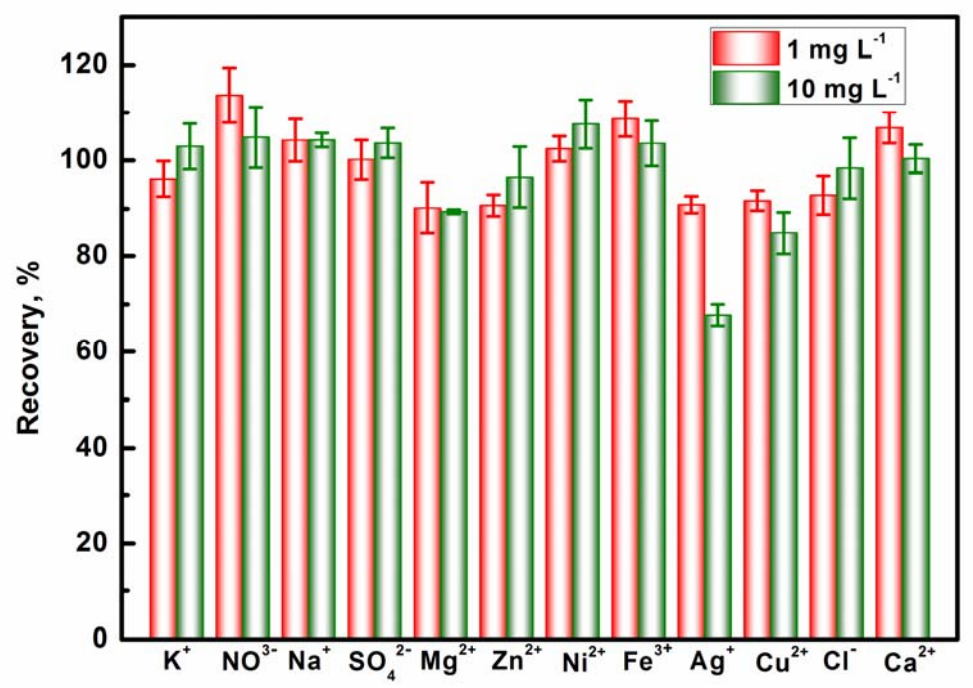

Figure S5. Effects of coexisting ions on the response from a 10 μg L^{-1} of Hg^{2+}.

7. Typical Calibration Curves for IHg and MeHg

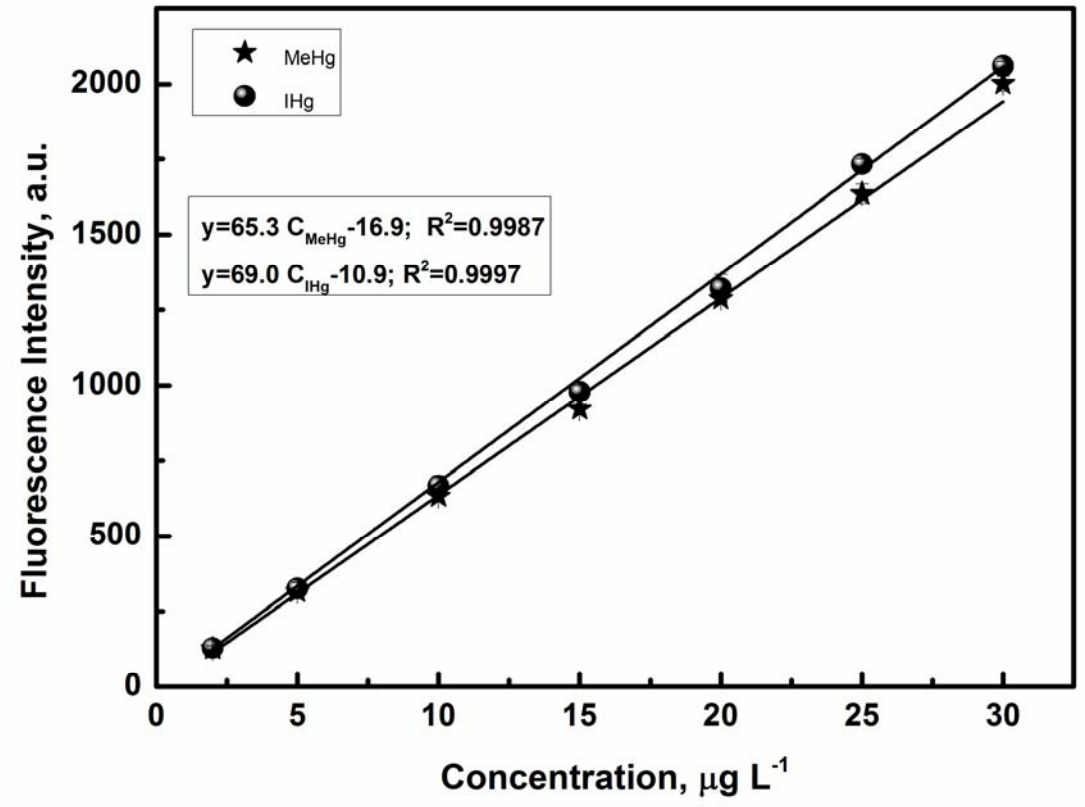

Figure S6. Typical calibration curves for IHg and MeHg

8. Repeatability of the Proposed Method

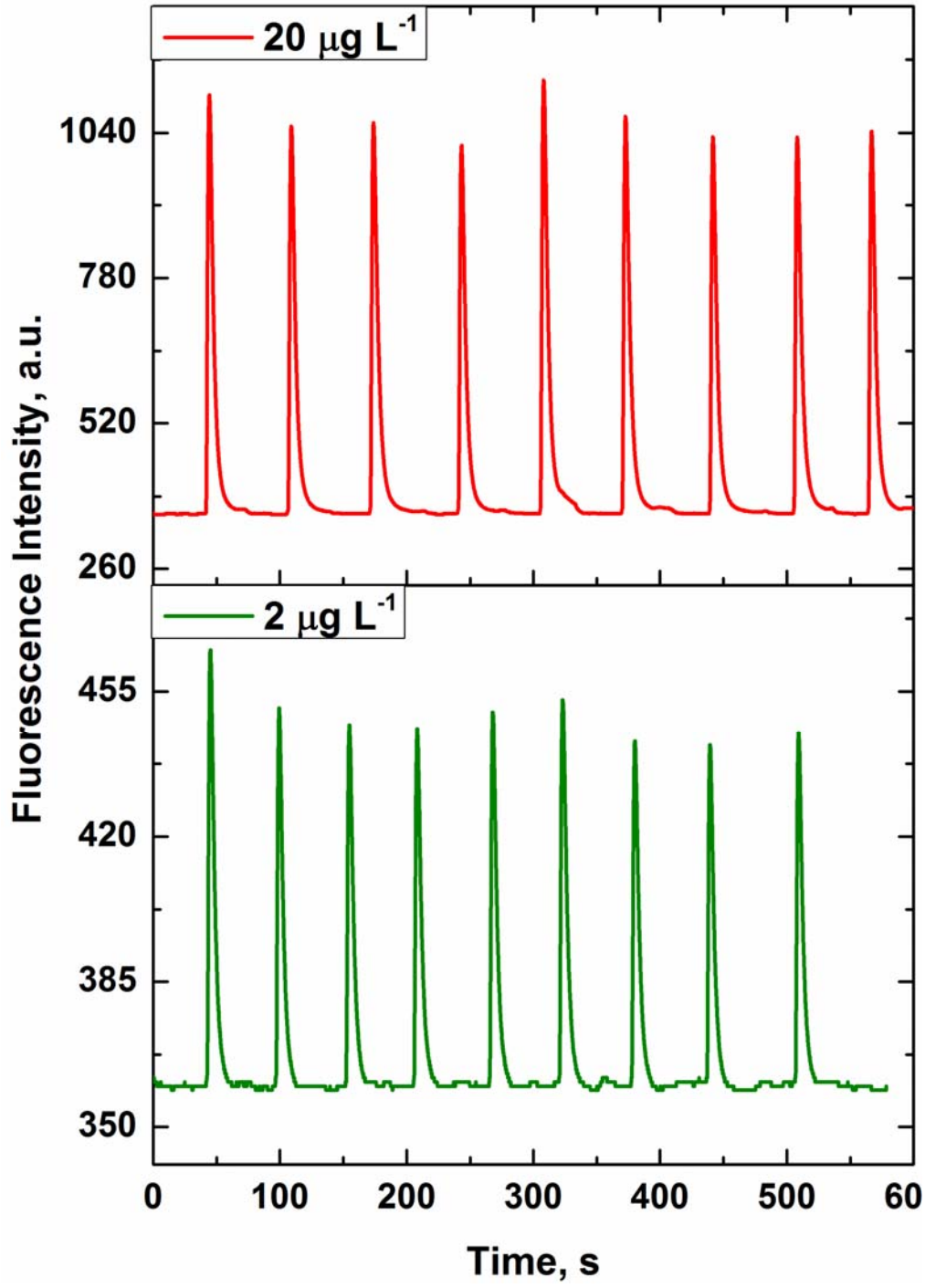

Figure S7. Signals obtained from repeat injections of solutions containing 2 and 20μg L^{-1} Hg^{2+}, respectively.

9. Comparison of the Memory Effects Obtained by Conventional CVG-AFS and FI-SD-SEGD-CVG-AFS

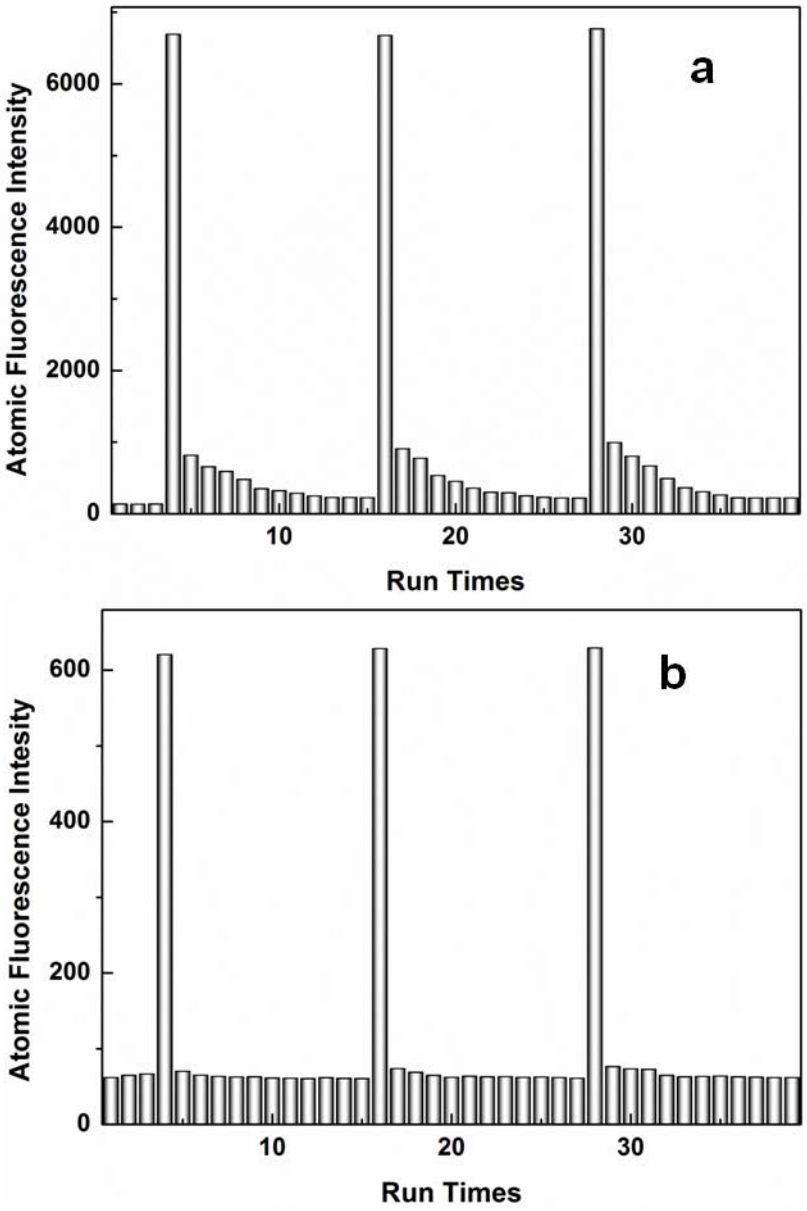

Figure S8. Memory effects obtained by conventional CVG-AFS (a) and FI-SD-SEGD-CVG-AFS (b).

REFERENCES

1. Wu, X.; Yang, W. L.; Liu, M. G.; Hou, X. D.; Zheng, C. B. *J. Anal. At. Spectrom.* **2011,** *26,* 1204-1209.
2. Zheng, C. B.; Li Y.; He, Y. H.; Ma, Q.; Hou, X. D. *J. Anal. At. Spectrom.* **2005,** *20,* 746-750.